

Microfluidics for generation and characterization of liquid and gaseous micro- and nanojets

Nisarga Naik^{a,*}, Christophe Courcimault^a, Hanif Hunter^b, John Berg^b, Jungchul Lee^b, Kianoush Naeli^a, Tanya Wright^b, Mark Allen^a, Oliver Brand^a, Ari Glezer^b, William King^b

^a School of Electrical and Computer Engineering, Georgia Institute of Technology, Atlanta, GA 30332-0405, United States

^b Woodruff School of Mechanical Engineering, Georgia Institute of Technology, Atlanta, GA 30332-0405, United States

Received 1 March 2006; received in revised form 17 April 2006; accepted 18 April 2006

Available online 27 June 2006

Abstract

This paper reports a microfluidic system for the generation and characterization of liquid and gaseous micro- and nanojets. The system comprises in-plane silicon micro/nanonozzles with dimensions ranging from 500 nm to 12 μm , a micro-to-macrofluidic interface and package, and a high pressure delivery source allowing microfluidic flow at pressure drops up to 15 MPa (2200 psi). Further, the system possesses the ability to characterize the jets by use of both shadowgraphy and impinging cantilever techniques. Unlike previous work reporting the fabrication of nano-orifices defined within the thickness of the substrates [1–4], the in-plane nanonozzles presented in this paper are designed to sustain the high pressures necessary to obtain substantial nanofluidic jet flows. This approach also allows important three-dimensional features of nozzle, channel and fluidic reservoir to be defined by design and not by fabrication constraints, thereby meeting important fluid-mechanical criteria such as a fully developed flow. The shrinking jet dimensions demand new metrology tools to investigate their flow behavior. A laser shadowgraphy technique is used to visualize and image the jet flows. Micromachined heated and piezoresistive cantilevers are used to investigate the thrust and heat flux characteristics of the jets. © 2006 Elsevier B.V. All rights reserved.

Keywords: Micro/nanonozzle; Micro/nanojet; KOH wet etching; Laser shadowgraphy; Cantilever

1. Introduction

With advancements in microfluidics, applications of micro/nanojets are expanding to a variety of areas, including ink jet printing [4], drug [5] and gene delivery, localized etching/nanofabrication [3], selective deposition [6] and microelectronic cooling [7]. In the past very little work has been reported on the generation and characterization of sub 10 μm liquid jets.

Previously work has been reported on fabrication of out-of-plane silicon micro/nanonozzles utilizing focused ion beam (FIB) milling of potassium hydroxide (KOH) etched hollow pyramids [1–3]. Materials other than silicon have been employed in some cases like generation of organic molecular nanojets by commercial glass pipettes of submicron orifice diameter [6,8] and polymeric nanonozzles fabricated by sacrificial template printing [9]. The above mentioned methods are not suitable

for high pressure applications, or involve serial fabrication processes that may make mass-manufacturing more difficult.

Based on previously reported work [10], the in-plane fabrication approach presented in this paper is designed to produce silicon nozzles capable of supporting large pressure drops required to drive micro/nanojets. Silicon is chosen as the material for this on account of its good mechanical properties and availability of many silicon-based microfabrication technologies. The entire nozzle unit is fabricated by a single mask step using anisotropic wet etching. All the dimensions and profiles are defined by the design giving maximum flexibility to meet design requirements. The aspect ratio of the cross section of nozzle channels is maintained very close to unity to ensure generation of stable circular jets. Apart from the simplicity of fabrication and flexibility of design, this approach offers a further advantage of ability to reduce the micromachined orifice dimensions to the submicron range very easily by controlled oxidative sealing.

Current trends in microfluidic miniaturization have led to an interest in examining the behavior of liquids at the nanoscale. In the absence of experiments that could directly measure liq-

* Corresponding author. Tel.: + 404 894 9908.
E-mail address: nisarga@gatech.edu (N. Naik).

uid flow at this scale, numerous studies have been focused on molecular dynamics simulations [11,12]. In this work, laser shadowgraphy is employed to visualize and image free liquid microjet flows. Piezoresistive and thermal cantilevers are used to characterize liquid and gaseous jets.

2. Micro/nanonozzle fabrication

The micro/nanojets are generated from micromachined silicon nozzles consisting of a nozzle channel and a small scale pressurized reservoir. Fig. 1 depicts the fabrication sequence of the nozzles. Silicon dioxide is grown on a double-side polished 450 μm thick (100) silicon wafer (Fig. 1a). Standard photolithography is performed to delineate the nozzle structure on one side of the wafer. The oxide layer is etched and patterned using inductively coupled plasma (ICP) etching (Fig. 1b). Anisotropic wet etching with potassium hydroxide (KOH) (concentration of KOH = 40% at 70 °C) is carried out to define channels and reservoirs in the silicon substrate (Fig. 1c). Using backside alignment, the other side of the wafer is patterned to facilitate the eventual individualization of the dies. The oxide layers are etched away using hydrofluoric (HF) acid and the

wafer is piranha cleaned. The nozzle structures are enclosed by fusion bonding with another silicon wafer, and the stack is annealed at 1100 °C for 4 hours (Fig. 1d). The nozzles are then individualized using a through-wafer ICP etch employing the Bosch process or alternatively by dicing (Fig. 1e). These separation techniques result in sidewall roughness. Fig. 2a illustrates the surface roughness due to ICP etching. This may have resulted due to redeposition of etched particles causing the formation of micromasks. Imperfections on the exit plane of the jets lead to instability of the jets. Fig. 3a and b show shadowgraph images of pooling and spraying of the jets necessitating a smooth surface. Hence the surface of the nozzles containing the orifice outlet is polished using chemical mechanical polishing (Fig. 2b). Oxidative sealing is then optionally utilized to reduce the openings of the nozzles from a few microns to the nanometer range (Fig. 1f). Fig. 4 shows a schematic of an individualized nozzle with enclosed channel and reservoir. This fabrication technology presents several interesting features. The entire nozzle structure, from the reservoir to the exit orifice is defined by photolithography, providing high design flexibility. Parameters such as channel length and width, and reservoir width and depth are easily alterable by design (Fig. 5a). The dimen-

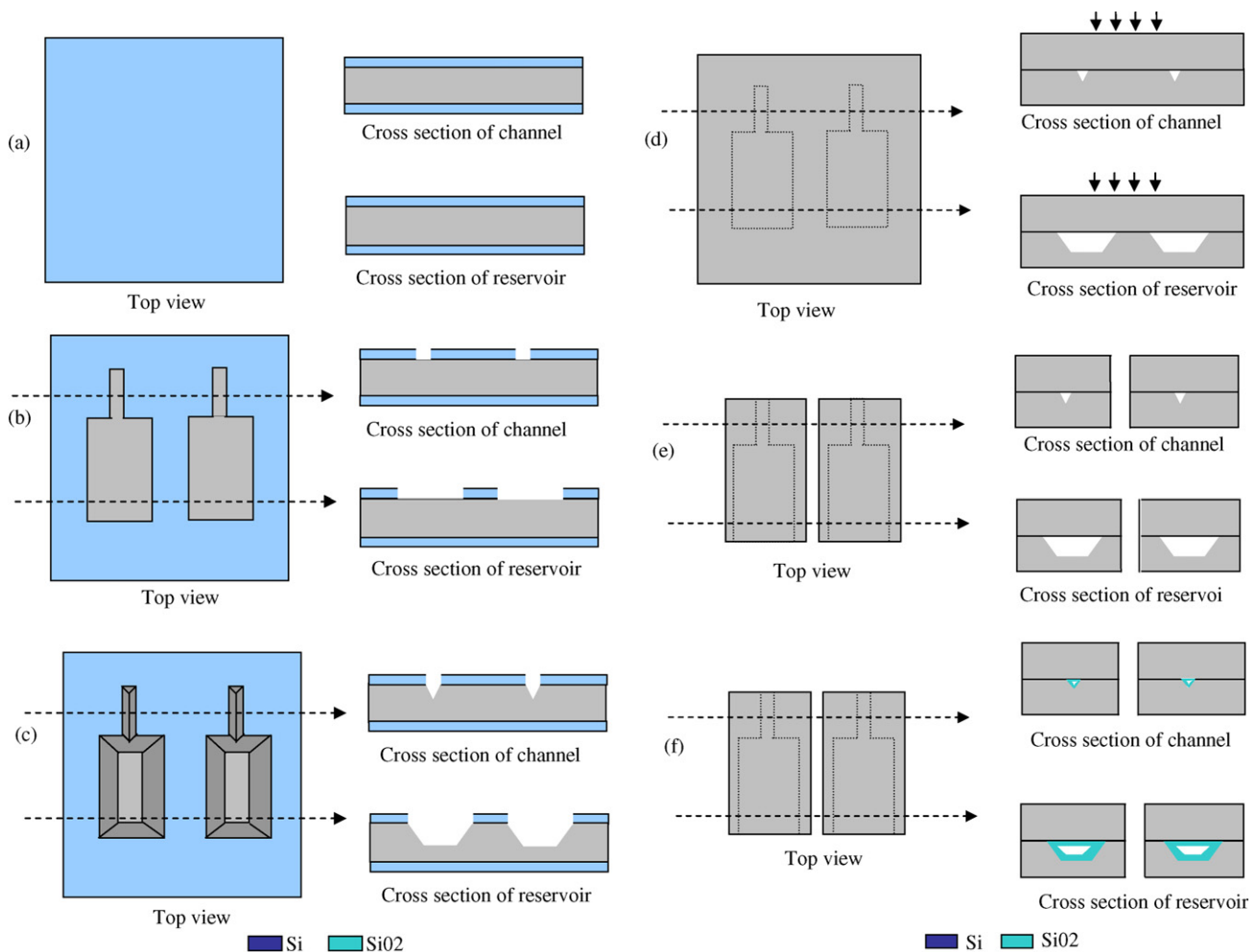


Fig. 1. Fabrication sequence: (a) silicon dioxide is deposited on both sides of the wafer, (b) silicon dioxide is patterned, (c) anisotropic wet etching is performed to etch the channel and the reservoir, (d) silicon to silicon fusion bonding is performed to enclose the nozzles, (e) dies are separated by through wafer silicon etch by ICP or dicing and (f) the nozzles are optionally oxidized to reduce the orifice dimension from micrometer to nanoscale.

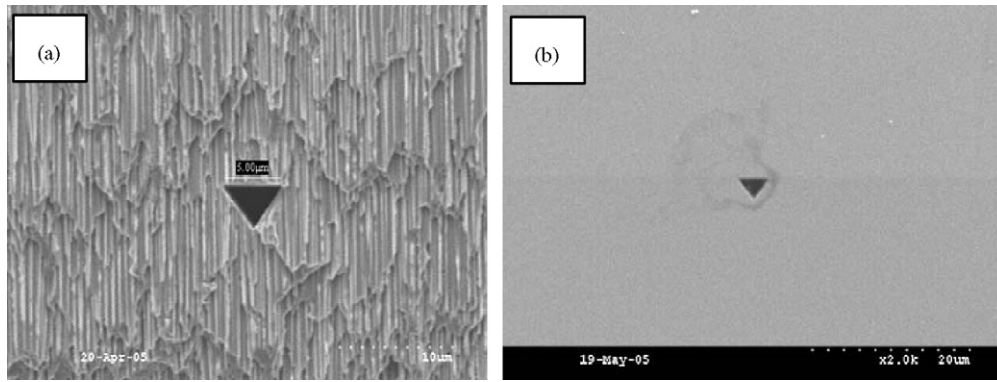


Fig. 2. The exit plane of the nozzle: (a) showing the surface roughness after an ICP etch is performed to separate the dies and (b) after performing chemical mechanical polishing (CMP) to smoothen out any fabrication imperfection.

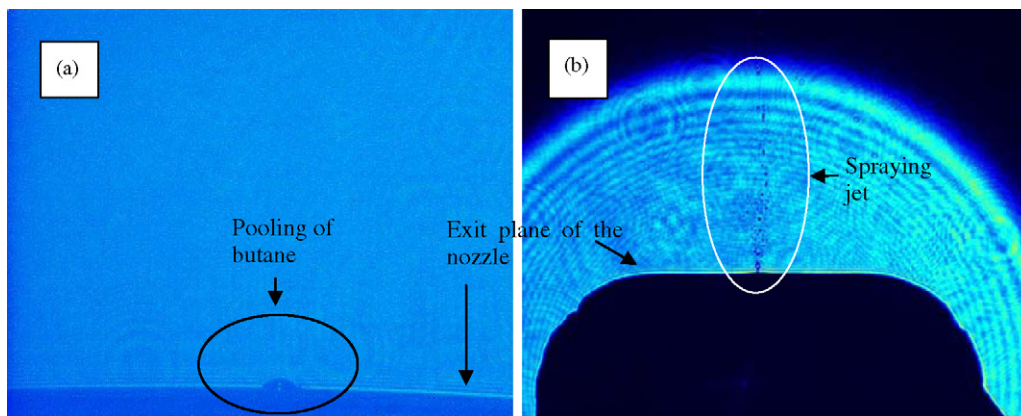


Fig. 3. Shadowgraph images of unstable jets caused due to fabrication imperfections on the exit plane of the nozzle illustrating: (a) pooling of butane on the surface of the nozzle and (b) spraying of butane rather than forming a column jet.

sions of the reservoir are chosen in order to minimize the surface area of the interior of the reservoir while obtaining a maximum possible entry (cross section) surface area for the fluid. This optimization reduces the reservoir surface area facing the fluid pressure, increasing the pressure withstanding capacity of the nozzle. The channel length is chosen to be 10-times the channel width in order to ensure generation of a fully developed flow.

In the above approach, a single anisotropic KOH wet etching step allows the definition of triangular channels with very small cross sections while etching a deeper reservoir. KOH etching exhibits interesting properties as it etches different silicon

crystal planes with different etch rates; for example, the (1 0 0) plane is etched 70-times faster than the (1 1 1) plane (concentration of KOH = 34% at 70.9 °C) [13]. This property allows the fabrication of structures of different depths using a single mask process (Fig. 5b). Since the line width of the channel is very small compared to the reservoir, the early intersection of (1 1 1) planes results in etch stop. We obtain a triangular channel with a very small cross section while the reservoir continues to etch. With a timed etch the required depth of the reservoir can be obtained. The (1 1 1) planes of the nozzle channel offer smooth walls for fluid flow. Also the undercut of convex corners and the ramp between the reservoir and the channel give a smooth transition for the fluid to flow from the reservoir to the orifice structure (Fig. 5a). For concentration of KOH = 40% at 70 °C, the undercut of convex corners (in x and y directions) is roughly 2.5-times the etch rate of the depth (z direction).

Thermal oxidation of individualized nozzles enables controlled reduction of orifice size from the micron range to the nanometer range. Fig. 6 shows a 460 nm nozzle obtained after a 16 hours long wet oxidation at 1100 °C of a 3 µm triangular nozzle. This step enables us to fabricate nanonozzles without resorting to nanolithography.

Variations of the above design can be obtained by adding another mask step. To obtain a rectangular cross section ori-

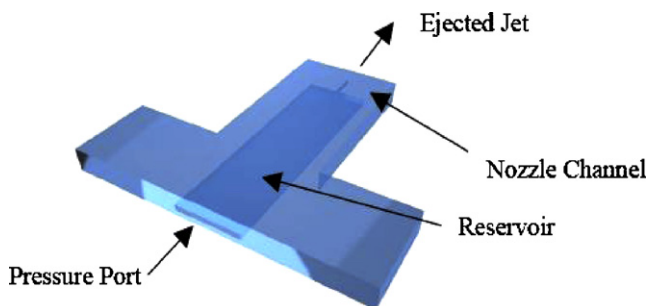


Fig. 4. 3D schematic of an individualized nozzle with fluid reservoir and nozzle channel.

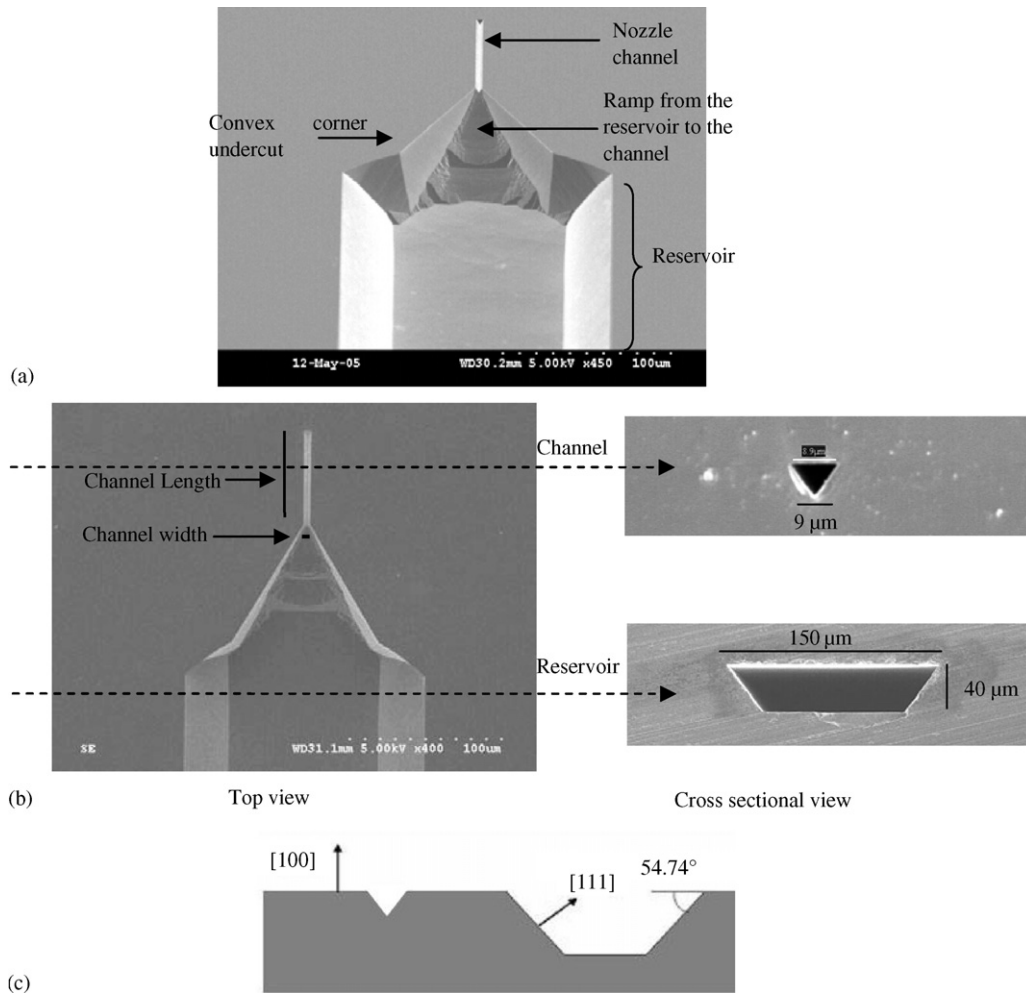


Fig. 5. SEM images of KOH etched nozzle: (a) tilted view showing different parts of the nozzle namely the channel, the reservoir and the ramp, (b) top view and cross sectional view and (c) schematic of KOH etch profile.

Since the reservoir is etched by KOH etching in order to obtain the smooth ramp; while the nozzle channel is etched by ICP etching as compared to KOH etching in the previous design (Fig. 7). In the case of KOH etched channels, a misalignment may lead to channel dimensions different than that designed in the mask as shown in the Fig. 8. An additional mask step assures reproducibility of nozzle-channel length. Fig. 9a shows

the cross section of a rectangular nozzle. The edges of the rectangle are rounded due to a slight isotropy of the ICP etch. A near-circular cross section channel can be obtained by oxidizing the triangular channel and etching the grown silicon dioxide with hydrofluoric acid. The oxidation rate towards the corners of the triangles is less compared to that along the rest of the edge, leading to a nonuniform oxide profile along the edge (Fig. 6b).

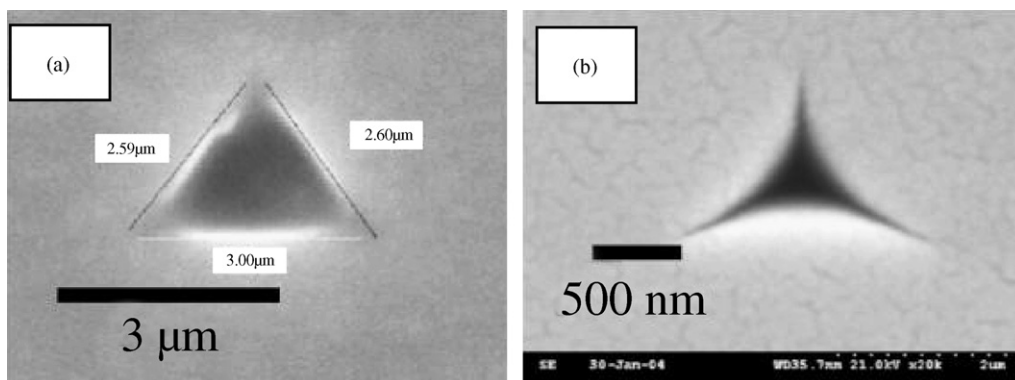


Fig. 6. SEM images of a 3 μm nozzle: (a) before oxidation, (b) after 16 hours of wet oxidation at 1100 °C.

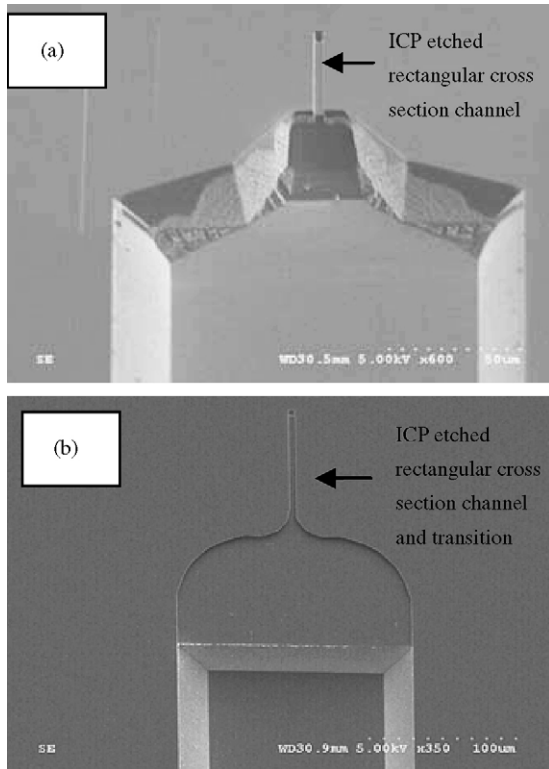


Fig. 7. SEM images of different nozzle designs fabricated using an additional mask step to build the channel and reservoir in different steps.

Thus, the corners are rounded off when the oxide is stripped (Fig. 9b).

3. Testing and characterization of micronozzles

After fabrication, the micro/nano nozzles are interfaced with a pressure generation apparatus using a machined stainless steel

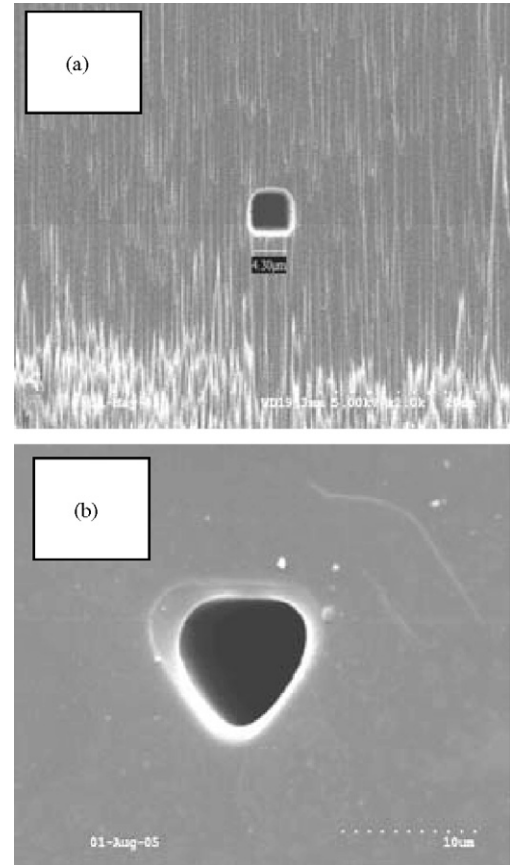


Fig. 9. SEM images of cross section of: (a) $4\text{ }\mu\text{m} \times 4\text{ }\mu\text{m}$ rectangular cross section nozzle, (b) $9\text{ }\mu\text{m}$ rounded triangular cross section nozzle obtained after oxidation of a $7\text{ }\mu\text{m}$ nozzle and stripping the oxide.

plate (Fig. 10). The working liquids are propane and butane (with surface tensions 0.0075 N/m and 0.0123 N/m , respectively, and vapor pressures 0.86 MPa and 0.22 MPa , respectively). A schematic of the pressurizing system is shown in Fig. 11. In

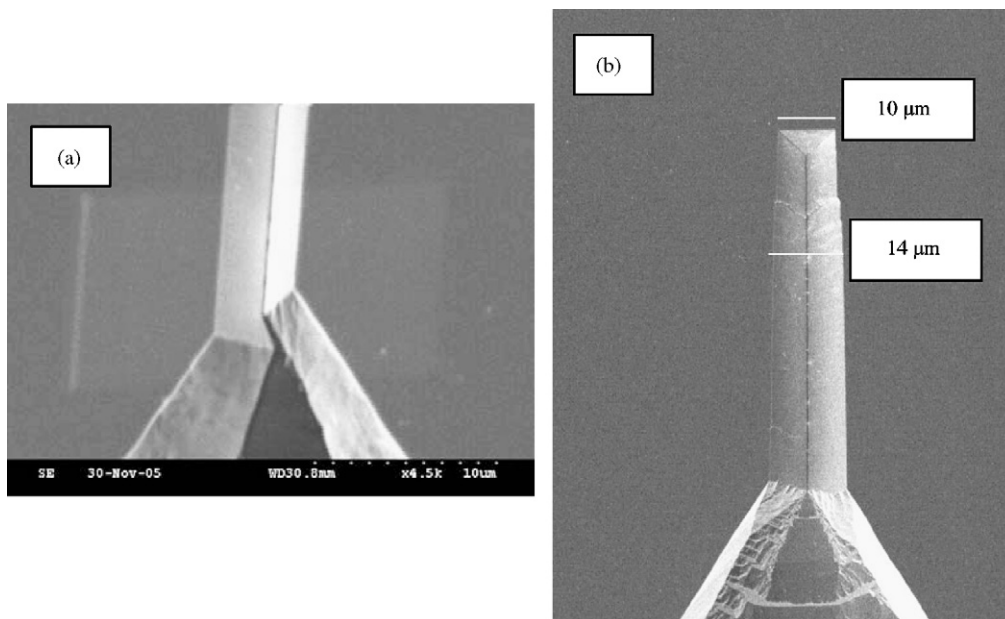


Fig. 8. Variations in: (a) channel length and (b) channel width, resulting from misalignment before anisotropic KOH etching.

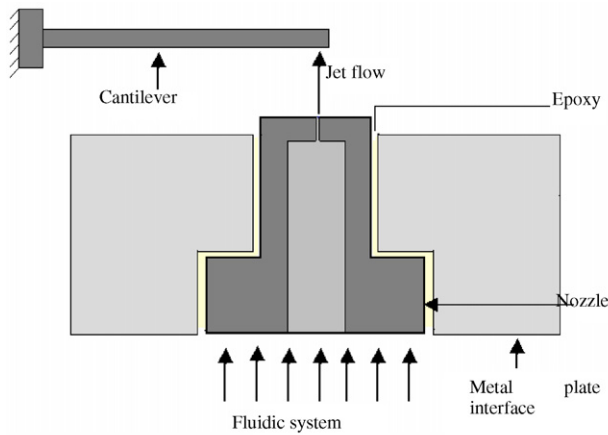


Fig. 10. Cross section schematic of metal plate and nozzle assembly showing jet impingement on the cantilever.

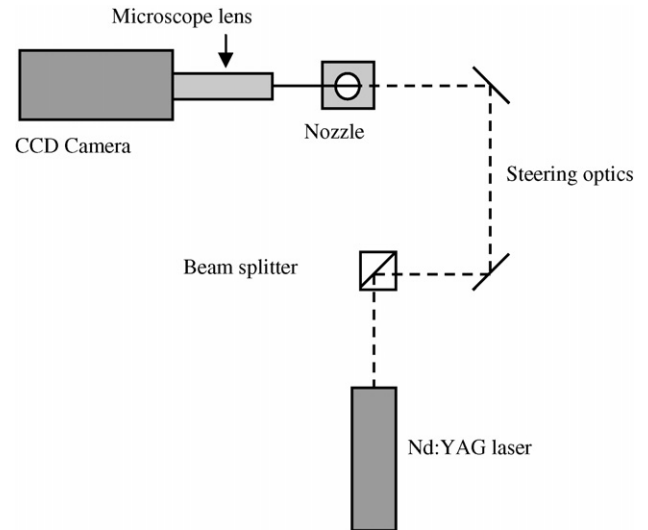
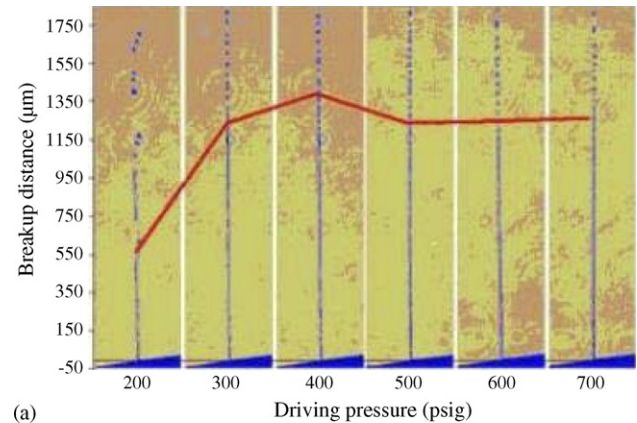


Fig. 12. Shadowgraphy setup schematic.

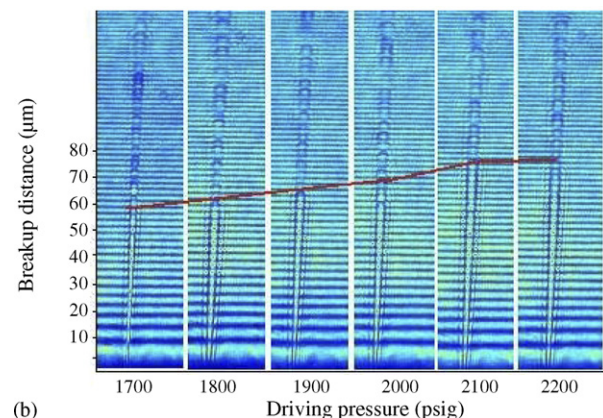
this system, nitrogen is used for pressurizing (up to 15 MPa (2200 psi)). Before the system is filled with the working fluid, it is first pressurized slightly above its vapor pressure using nitrogen, and then the liquid (propane or butane) is pumped into the reservoir to the desired level. The system is then pressurized using nitrogen (above the liquid level) to the desired working pressure. Fig. 12 shows a schematic of the jet visualization and imaging setup. The micro-nano jets are visualized by laser shadowgraphy. The flow field is illuminated using a (double-pulse) Nd:YAG laser (532 nm). Instantaneous images of the flow are captured using a PIV CCD camera.

Pressures ranging from 0.34 MPa (50 psi) to 15 MPa (2200 psi) are applied to expel liquid butane and propane jets from nozzles with dimensions varying from 500 nm to 12 μm . It is observed that jets breakup into droplets at a certain distance from the exit plane. Fig. 13a and b show shadowgraphy images of 12 μm and 1 μm jets, respectively, illustrating the variation of jet breakup distance with driving pressures. It is observed that at lower driving pressures the breakup occurs closer to the orifice while at higher driving pressures it occurs further downstream. The noted inconsistency in the 12 μm driving pressures

may be due to bubble formation at the exit of the jet. Another observation can be derived from these graphs. If we normalize the breakup distance with the jet dimension for the 12 μm jet, we get a value close to 50 at 200 psi. The same analysis for the 1 μm jet gives a value close to 60 at 2000 psi, i.e. at one-order higher pressure. This shows that the jets are similar in



(a)



(b)

Fig. 13. Shadowgraphs showing variation of jet breakup distance with driving pressure of: (a) a 12 μm jet and (b) a 1 μm jet.

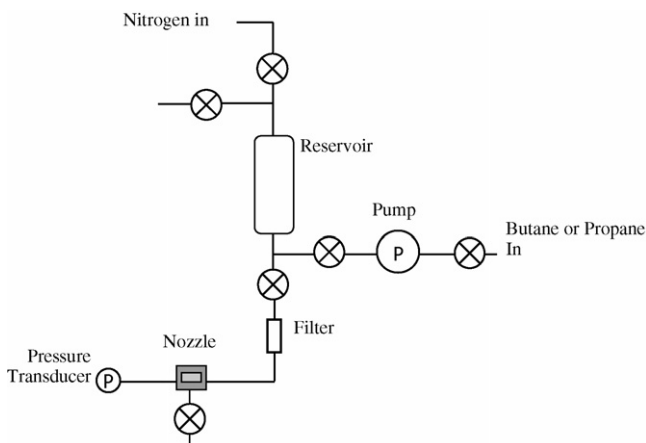


Fig. 11. Fluidic system schematic.

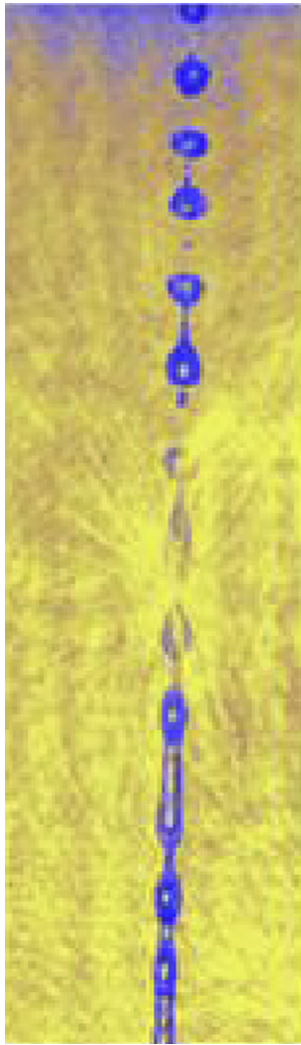


Fig. 14. Spacing between successive droplets varies suggesting presence of multiple frequencies.

nature. Close up images of the jet breakup domain show that at ambient pressure, the streamwise spacing between successive droplets varies suggesting the presence of multiple frequencies (Fig. 14).

The velocity of the atomized droplets is estimated over a range of driving pressures by cross-correlation of identifiable droplet images in successive frames that are taken at a given time delay. For a $6\text{ }\mu\text{m}$ nozzle, jet velocities ranging from 40 m/s to 60 m/s are obtained for reservoir pressures ranging from 600 kPa (94 psi) to 1400 kPa (203 psi) (Fig. 15).

The micro/nanojets are also characterized, in terms of velocity, thrust and heat flux coefficients, using novel metrology tools such as piezoresistive and thermal cantilevers. The piezoresistive cantilever is scanned over the nozzle exit plane at $1\text{ }\mu\text{m/s}$ rate (Fig. 10). The jet impinging on the tip of the cantilever causes it to deflect, the deflection being measured by a resultant voltage imbalance produced in a Wheatstone bridge connected to the cantilever. With this data, the thrust and hence the velocity of the jet are calculated. In addition to this, these

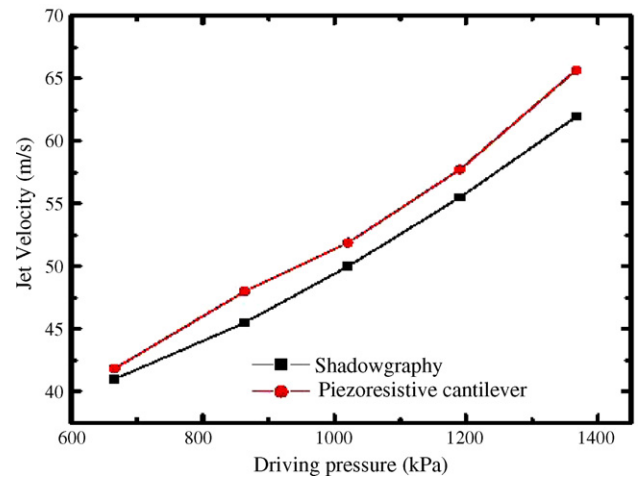


Fig. 15. Velocity measurement of a $6\text{ }\mu\text{m}$ jet using shadowgraphy and a piezoresistive cantilever.

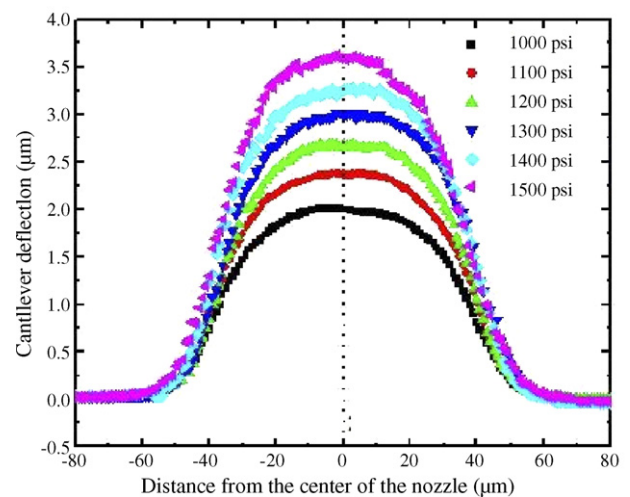


Fig. 16. Cantilever deflection as it is scanned over a $2.5\text{ }\mu\text{m}$ nozzle with a nitrogen jet flow.

cantilevers are also used to determine if the submicron nozzles are clogged or not since it is difficult to image jets on these scales. Fig. 16 indicates change in cantilever deflection as it is scanned over a $2.5\text{ }\mu\text{m}$ nozzle with a nitrogen jet flow at different pressures. Since a gaseous jet spreads out, the velocity of the jet cannot be determined. A butane jet, $6\text{ }\mu\text{m}$ in diameter is characterized with respect to thrust and velocity [14]. Fig. 15 compares the velocity data for the jet obtained by imaging technique and the piezoresistive cantilever.

4. Nanojet realization

A propane jet was obtained from a 500 nm nozzle at 12 MPa (1750 psi). The jet was imaged using an overhead CCD camera (Fig. 17). Though detailed data was not obtained due to the necessity to further develop appropriate metrology tools, this result demonstrates the feasibility of generating nanojets using this approach.

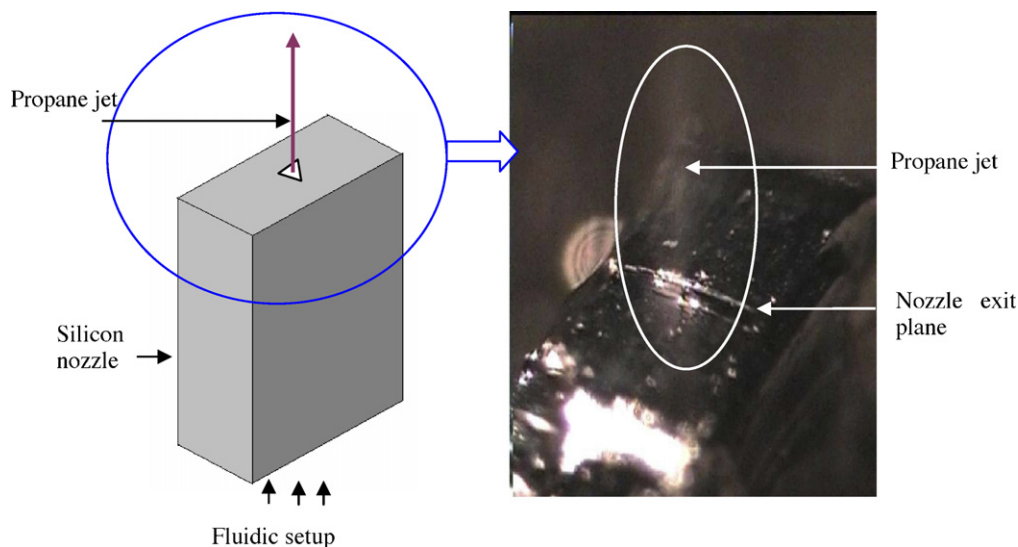


Fig. 17. Image of a propane jet generated from a 500 nm nozzle.

5. Conclusion

Micronozzles have been fabricated by a single mask step and then oxidatively sealed to form orifices in the submicron range. This fabrication technique offers high design flexibility as well as application of large pressures. The shapes and dimensions of the nozzle channel and reservoir can be easily modified as per application requirements. The presented approach has the potential for further advancements towards sub-100 nm jets. These nozzles ranging from 500 nm to 12 μm have been able to successfully generate stable liquid and gaseous jets and withstand the pressures required to drive them. Laser shadowgraphy has been employed to visualize and image these jets. Metrology tools such as piezoresistive and thermal cantilevers have been utilized to characterize the jet flow.

Acknowledgements

We would like to thank Mr. Richard Shafer, Dr. Bruno Frazier, Mr. Mason Graff, Dr. Thayne Edwards and Mr. Vinh Nguyen of Georgia Institute of Technology for their great support on the project. This project was partially supported by NSF Nanoscale Interdisciplinary Research Teams (under contract # CTS-0304009).

References

- [1] J. Voigt, F. Shi, K. Edinger, P. Guthner, I.W. Rangelow, Nanofabrication with scanning nanonozzle 'Nanojet', *Microelectron. Eng.* 57 (2001) 1035–1042.
- [2] J. Voigt, F. Shi, P. Hudek, I.W. Rangelow, K. Edinger, Progress on nanostructuring with nanojet, *J. Vacuum Sci. Technol. B (Microelectr. Nanometer Struct.)* 18 (6) (2000) 3525–3529.
- [3] I.W. Rangelow, J. Voigt, K. Edinger, NANOJET: Tool for the nanofabrication, *J. Vacuum Sci. Technol. B (Microelectr. Nanometer Struct.)* 19 (6) (2001) 2723–2726.
- [4] L. Palm, L. Wallman, T. Laurell, J. Nilsson, Development and characterization of silicon micromachined nozzle units for continuous ink jet printers, *J. Imag. Sci. Technol.* 44 (6) (2000) 544–551.

- [5] G.H. Wang, Z.Y. Zhou, Y.Y. Feng, X.Y. Ye, A single-nozzle microjet for drug delivery, *Proc. Int. Symp. Test. Measure.* 1 (2003) 145–148.
- [6] M. Goto, L.V. Zhigilei, J. Hobley, M. Kishimoto, B.J. Garrison, H. Fukumura, Laser expulsion of an organic molecular nanojet from a spatially confined domain, *J. Appl. Phys.* 90 (9) (2001) 4755–4760.
- [7] E.N. Wang, L. Zhang, L. Jiang, J.-M. Koo, J.G. Maveety, E.A. Sanchez, K.E. Goodson, T.W. Kenny, Micromachined Jets for Liquid Impingement Cooling of VLSI Chips, *J. Microelectromech. Syst.* 13 (5) (2004) 833–842.
- [8] M. Goto, S. Kawanishi, H. Fukumura, Laser implantation of dicyanoanthracene in poly(methyl methacrylate) from a 100-nm aperture micropipette, *Appl. Surf. Sci.* 154 (2000) 701–705.
- [9] S. Wang, C. Zeng, S. Lai, Y. Juang, Y. Yang, J. Lee, Polymeric nanonozzle array fabricated by sacrificial template imprinting, *Adv. Mater.* 17 (9) (2005) 1182–1186.
- [10] N. Naik, C. Courcimault, H. Hunter, J. Berg, J. Lee, K. Naeli, T. Wright, M.G. Allen, O. Brand, A. Glezer, W.P. King, Fabrication and characterization of liquid and gaseous micro-and nanojets, *Proc. ASME IMECE, FL, USA* (2005).
- [11] M. Moseler, U. Landman, Formation, stability, and breakup of nanojets, *Science* 289 (5482) (2000) 1165–1169.
- [12] J. Eggers, Dynamics of liquid nanojets, *Phys. Rev. Lett.* 89 (8) (2002), 084502-1–4.
- [13] M. Shikida, K. Sato, K. Tokoro, D. Uchikawa, Differences in anisotropic etching properties of KOH and TMAH solutions, *Sens. Actuators A (Phys.)* A80 (2) (2000) 179–188.
- [14] J. Lee, K. Naeli, H. Hunter, J. Berg, T. Wright, C. Courcimault, N. Naik, M.G. Allen, O. Brand, A. Glezer, W.P. King, Micro-cantilever based metrology tool for flow characterization of liquid and gaseous micro/nanojets, *Proc. ASME IMECE, FL, USA* (2005).

Biographies

Nisarga Naik received the BS in electrical engineering from V.J.T.I, Mumbai University, India in 2003. She is currently working towards her PhD at Georgia Tech. Her research involves fabrication and characterization of nanonozzles.

Christophe Courcimault received the French equivalent of a BS degree in physics from INSA Toulouse and the French equivalent of a PhD degree in microelectronics and micro engineering from the same school, in June 2005. His research, focusing on the development of microsystems for the fabrication of nanosystems, was carried out at the Georgia Institute of Technology in Atlanta, GA. After graduating in June 2005, he joined the R&D Department of a biomedical Atlanta-based company, CardioMEMS, Inc., where he develops implantable wireless pressure sensor.

Hanif Hunter received the BS in mechanical engineering from Georgia Institute of Technology in 2002. He is currently working towards a PhD at Georgia Institute of Technology. He is studying and characterizing micro and nanoscale jets.

John Berg received the BS in mechanical engineering from Johns Hopkins University, Baltimore, Maryland in 2003. He worked toward his PhD in mechanical engineering at Georgia Tech from 2003–2004 before leaving engineering to pursue a career in clinical psychology. He is currently working toward his PhD in clinical psychology at Emory University, Atlanta, Georgia.

Jungchul Lee received the BS and MS degree in mechanical engineering from Seoul National University, Seoul, Korea in 2001 and 2003, respectively. He is currently working toward the PhD degree at Georgia Institute of Technology. He is developing micromachined thermal sensors and actuators and investigating thermal transport in micro/nanoscale devices.

Kianoush Naeli received the BS degree in electrical engineering from Sharif University of Technology, Iran, in 1999 and the MS degree in electronics from the University of Tehran, Iran, in 2001. Currently he is a doctoral candidate in the Department of Electrical and Computer Engineering at Georgia Institute of Technology, where his research is focused on cantilever-based sensors.

Tanya Wright received her BS in mechanical engineering from Iowa State University, Ames, Iowa in 1999. After 3 years with Motorola in their automotive electronics division, she attended the Georgia Institute of Technology where she received a MS in mechanical engineering in 2005. Her thesis focused on the fabrication of heated micro-cantilevers. She is currently working for Schlumberger in their product center in Paris, France.

Mark Allen received the BA degree in chemistry, the BSE degree in chemical engineering, and the BSE degree in electrical engineering from the University of Pennsylvania, University Park, and the SM and PhD degrees from the Massachusetts Institute of Technology, Cambridge, in 1989. He joined the faculty of the Georgia Institute of Technology, Atlanta, in 1989, where he currently holds the rank of professor and the J.M. Pettit professorship in microelectronics. He is North American Editor of the *Journal of Micromechanics and Microengineering*. His research interests are in the areas of micromachining and microelectromechanical systems (MEMS); in particular, the development and application of new fabrication technologies for micromachined devices and systems. Dr. Allen was General Co-Chair of the 1996 IEEE MEMS Conference.

Oliver Brand received the MS degree in physics from the Technical University Karlsruhe, Germany, in 1990 and the PhD degree from ETH Zurich, Switzerland, in 1994. From 1995 to 1997, he was a postdoctoral fellow at the Georgia Institute of Technology (Georgia Tech), Atlanta. From 1997 to 2002, he worked at the Physical Electronics Laboratory (PEL), ETH Zurich, Zurich, Switzerland, as lecturer and group leader. In January 2003, he joined the Electrical and Computer Engineering Faculty, Georgia Tech. His expertise is in the areas of CMOS-based microsystems, MEMS fabrication technologies, and microsystem packaging.

Ari Glezer received the BS degree from Tel Aviv University, Israel, in 1974 and the MS and PhD degrees from the California Institute of Technology, Pasadena, in 1975 and 1981, respectively. Prior to joining the faculty of the Georgia Institute of Technology (Georgia Tech), he was a faculty of the University of Arizona. He joined Georgia Tech in 1992, where he currently holds the rank of professor and the George W. Woodruff Chair in Thermal Systems. His research interests focus on the manipulation and control of shear flows in a broad range of applications, including reacting and nonreacting mixing processes, enhancement of the aerodynamic performance of airborne and underwater vehicles, small-scale combustion-driven power systems, jet thrust vectoring and noise reduction, fluidic-driven heat transfer with an emphasis on electronic cooling, fluid atomization, and the development of novel fluidic actuator technologies including MEMS based actuators.

William P. King received the BS degree in mechanical engineering from the University of Dayton in 1996 and the MS and PhD degrees in mechanical engineering from Stanford University, Stanford, CA, in 1998 and 2002, respectively. Between 1999 and 2001, he spent 16 months in the Micro/NanoMechanics Group of the IBM Zurich Research Laboratory. In July 2002, he joined the faculty of the Woodruff School of Mechanical Engineering at the Georgia Institute of Technology (Georgia Tech), Atlanta, as assistant professor. At Georgia Tech, his group works on thermal engineering of micro/nanomechanical devices, including thermomechanical data storage and nanoscale thermal processing. He is the winner of the NSF CAREER award (2003) and the DOE PECASE award (2005).